ELSEVIER

Cement and Concrete Composites **20** (1998) 263–381
0958-9465/98/$ — see front matter

PII:S0958-9465(98)00018-3

Corrosion of Reinforcement Steel Embedded in High Water–cement Ratio Concrete Contaminated with Chloride

A. K. Suryavanshi,[a]* J. D. Scantlebury[b] & S. B. Lyon[b]

[a]Civil Engineering Department, NUS, Singapore, 119260
[b]Corrosion and Protection Centre, UMIST, Manchester, M60 1QD, UK

(Received 2 May 1997; accepted 23 March 1998)

Abstract

The aim of this investigation was to examine the role of internal chloride on the corrosion behaviour of steel in ordinary Portland cement (OPC), and sulphate resistant Portland cement (SRPC) mortar mixes of higher water–cement (w/c) ratios. For this purpose, the steel electrodes embedded in mortar specimens were subjected to short-term electrochemical monitoring. On completion of electrochemical monitoring, pore solution was extracted from the specimens for analysis. For the purpose of comparison, pore solution was also extracted from separate OPC and SRPC cylindrical mortar specimens hydrated in an environment isolated from the atmosphere. Results from microanalysis using scanning electron microscope (SEM) are also reported. The results demonstrated that mortars prepared with a cement of high tricalcium aluminate (C_3A) content, even when the w/c ratio of the mix was maintained at 0.70, still passivated the steel embedded in it even in the presence of chloride as high as 1% by weight of cement. Under a similar condition, the steel embedded in mortar prepared with a cement of low C_3A content was unable to passivate the steel electrode. The special protection mechanism by the lime-rich layer as proposed by Page for low w/c ratio concretes is also valid for the steel embedded in high w/c ratio mortar. The type of exposure condition (e.g. exposure to atmosphere) during the hydration period strongly influences the hydroxide ion concentration in the pore solution, while this has no effect on the free-chloride concentration in the pore solution. This study reconfirms the significance of the C_3A phase of cement in respect to chloride-binding processes.

Keywords: corrosion, chloride, pore solution, durability

Abbreviations: R_s: solution resistance, C_{dl}: double layer capacitance, ω: angular frequency, Z″: imaginary impedance, Z′: real impedance, R_{ct}: charge transfer resistance, |Z|: modulus of impedance, μf: micro Farad, Hz: Hertz, Ω: Ohm, SCE: saturated calomel electrode.

INTRODUCTION

In recent years, the long-term durability of concrete structures has become a matter of concern, primarily because of the corrosion of reinforcement steel. The reinforcement steel in concrete normally exhibits a high degree of corrosion resistance owing to the formation of an electrochemically stable passive film on its surface under appropriate conditions (pH and electrode potential). However, chloride ions derived from admixtures that are deliberately added during mixing, and also those originating from aggregates/mixing water (internal chloride), or those transported into the cover

*To whom correspondence should be addressed.

during exposure to aggressive chloride-bearing environment (external chloride), may depassivate the reinforcement steel surface to initiate pitting corrosion.

Although chloride is generally detrimental to the steel in concrete, only the unbound chloride (free-chloride) beyond a certain threshold level is responsible for the corrosion of the reinforcement steel. A part of the chloride present in OPC (ordinary Portland cement) concrete chemically binds during the hydration process to form the chloro-complex, Friedel's salt ($3CaO.Al_2O_3.CaCl_2.10H_2O$), depending on the amount of tricalcium aluminate (C_3A) phase present in the OPC. For example, OPC containing 9.5% C_3A by weight binds almost 1.6 times more chloride than a cement that contains 2.8% C_3A by weight,[1] and hence, cements rich in C_3A phase (e.g. OPC) are recommended for structures in coastal and marine environments. Although chloride binding ability is lowered in cements that are poor in C_3A phase, most chloride may still bind as a chloroferrite phase ($3CaO.Fe_2O_3.CaCl_2.10H_2O$), analogous to Friedel's salt.[2] Although cements that contain higher amounts of alkali metals (Na and K) are beneficial in raising the pH of the pore solution, they are known to inhibit the binding of chloride.[3,4] Similarly, when sulphate is present in substantial quantities it can decrease the amount of bound chloride, and thereby increase the risk of corrosion of the steel.[5] The source of chloride (internal or external) in concrete also has a significant role on the corrosion of reinforcement steel. For a given C_3A and chloride content, more chloride is bound if it is present in the mix from the time of mixing (internal chlorides) compared with when it penetrates the concrete from an external environment during the service life of a structure (external chloride).[3,6] Thus, from the corrosion point of view, chloride that penetrates from the external environment is generally more detrimental than chloride that is added during mixing. In both internal and external chloride-induced corrosion of steel reinforcement, the pore structure of the concrete plays a crucial role, by controlling the mobility of free-chloride ions.

The aim of this study is to examine the role of internally added chloride on the corrosion behaviour of steel in OPC and sulphate-resistant Portland cement (SRPC) mortars of higher water–cement (w/c) ratios. It is well known that the concretes of low w/c ratios (0.45) possess a greater resistance against atmospheric carbonation and chloride attack because of their dense pore structure. Apart from this, it is also reported that steel electrodes in low w/c ratio concretes derive an enhanced protection against corrosion through the lime-rich layer formed at the steel–mortar interface.[7] Thus, by knowing the inherent capabilities of low w/c ratio OPC concrete against chloride and carbonation-induced corrosion of steel reinforcement, the extent of corrosion resistance of steel in concrete/mortars of higher w/c ratios (> 0.45) can be determined. The selection of the higher w/c ratio is also justified, as ready-mixed concretes delivered to the site are often found to exceed the generally recommended w/c ratio of 0.45.[8] In the present investigation, the steel electrodes in OPC and SRPC specimens cast with mortar mixes of higher w/c ratios were subjected to short-term electrochemical impedance and electrochemical potential monitoring. On completion of electrochemical monitoring, the pore solution was extracted from the OPC and SRPC mortar specimens. This was done in order to verify the correlation that existed between the electrochemical results and the pore solution characteristics. For the purpose of comparison, pore solution was also extracted from separate OPC and SRPC cylindrical mortar specimens that were hydrated in an environment isolated from the atmosphere. Scanning electron microscopy (SEM) and energy dispersive analysis by X-rays (EDX) studies were also carried out to describe the steel–mortar interface, and also to identify the chloride-bearing phases that form in OPC and SRPC mortars.

EXPERIMENTAL WORK

As part of the experimental work, electrochemical studies (impedance spectroscopy, potential measurements), pore solution studies and microscopic analyses (SEM and EDX) were carried out as described below.

Electrochemical studies

For electrochemical studies, mortar specimens ($68 \times 28 \times 69$ mm) as shown in Fig. 1 were prepared with mortar mixes that contained

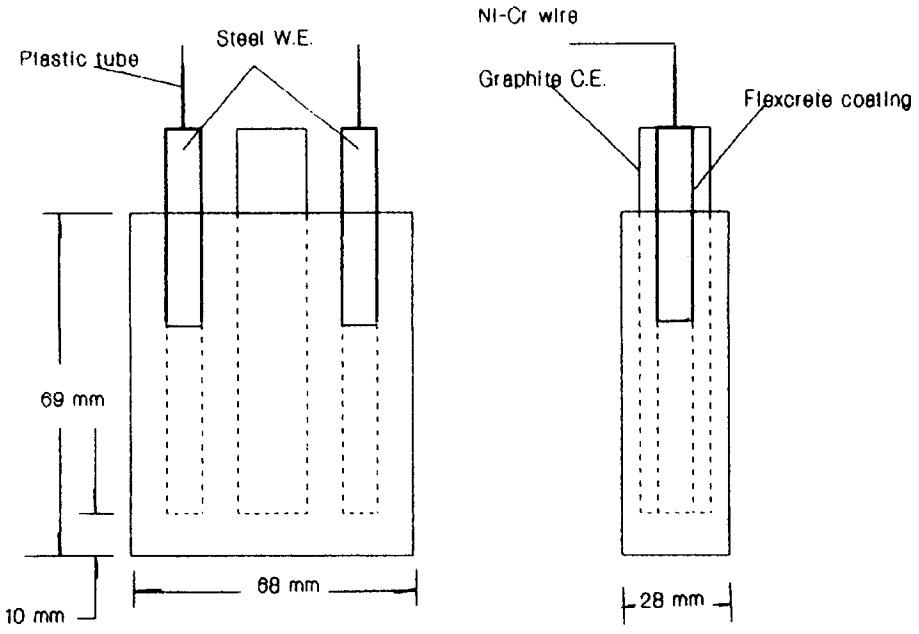

Fig. 1. A schematic diagram of the mortar specimen used for electrochemical studies.

different levels of chloride. Each mortar test specimen, as shown in Fig. 1, had two identical mild steel working electrodes of 7.9 mm diameter, and a high purity graphite electrode of 12.5 mm diameter, placed between the two steel electrodes. The mortar specimens were cast in a perspex mould that was specially designed to cast the specimens in an inverted position. This arrangement was necessary to avoid the formation of a bleeding pocket beneath the steel electrode surfaces when the specimen was cast in a normal way.

All the specimens were cast with OPC and SRPC mortar mixes of a 0.70 w/c ratio. In the present investigation, a w/c ratio of 0.70 was deliberately chosen in order to study the behaviour of steel embedded in mortars of higher w/c ratio than the generally recommended w/c ratio of 0.45. Mortar was used in lieu of concrete as the former is relatively more convenient for casting smaller specimens. The cement content of the mix was 400 kg m^{-3}, and the aggregate:cement ratio by weight was maintained at 4.0. The C_3A contents by weight percent for OPC and SRPC were 11.2% and 1.4%, respectively. Sodium chloride was added at the time of mixing at three different levels: 1%, 1.75% and 3.5% of chloride by weight of cement. The addition of 1.75% chloride by weight of cement as sodium chloride to the mix water, approximately simulates the condition of using sea water as mix water, and the other chloride levels chosen are above and below this 1.75% chloride level.

In all mortar specimens, polished steel electrodes of 7.9 mm diameter were used as working electrodes. The steel electrodes were polished on a bench drilling machine with emery papers in ascending order of 220, 400, 600, 800 and 1200 grades. To avoid crevice attack on the steel electrodes at the mortar–air interface, the steel electrode surface was partially coated with a polymer–cement-based coating system (Flexcrete 851) before embedding them in mortar to a depth of 24 mm below the mortar–air interface as shown in Fig. 1. After curing the coating for 24 hours, the loosely adhering lip of the coating towards the exposed surface was cut (1–2 mm in length) with a scalpel all around the circumference to avoid the formation of potential crevice sites. Thus, the steel electrodes after partially coating as described above had an exposed surface area of 9.2 cm^2.

The mortar specimens were demoulded 24 hours after casting, and were immediately subjected to potential and alternating current (AC) impedance monitoring. AC impedance was chosen because this technique has the advantage of providing information on the electrodic processes that occur at the steel–mortar interface, in addition to the kinetics of the reactions.

After the electrochemical tests, the specimens were aged in a humidity chamber that was maintained at an average relative humidity (RH) of ≈85% until around the 70th day after casting. In order to avoid the leaching of the ionic species from the specimens, especially the chloride ions, the above method of curing was preferred over the normal method of soaking in water. The specimens were then taken out of the humidity chamber for periodic electrochemical monitoring until around the 70th day after casting the specimen.

The electrochemical potential of the steel electrode was measured using a gel salt bridge (agar+sodium chloride) with a saturated calomel electrode (SCE) on the mortar surface directly above the steel electrodes. A piece of paper (1 cm^2) soaked in deionized water was additionally placed between the mortar and the salt bridge to improve the electrolytic contact. In order to avoid the current flow through the measuring circuit, a voltmeter (Keithley Electrometer, model: 610C) of high input impedance (10^{14} Ohms) was used for measuring the potentials. The intervals chosen for the periodical electrochemical monitoring were based on the rate of hydration of the cement, with more frequent intervals until around the 40th day of hydration, and less frequent intervals from then onwards.

In the present investigation, the impedance was measured using a four-channel Solartron (type 1254) digital frequency response analyser (FRA) interfaced to a potentiostat. Data were logged using a microcomputer for subsequent analyses. A standard commercial software package, Procomm, was used for data logging. The impedance was measured by imposing a sinusoidal voltage perturbation of 10 mV peak-to-peak amplitude (7 mV rms value) with a frequency that varied between 10 and 40 mHz on the working electrode held at its corrosion potential. The impedance measurements were carried out by adopting the three-electrode method for each of the steel electrodes of the specimen, by making the central graphite electrode the common counter electrode. The reference electrode used in the three-electrode system circuit has been shown to interfere in the high frequency (kHz) impedance spectra;[9] however, for the steel–concrete system this would not affect the results as the majority of the electrode response is derived from frequencies well below 100 Hz. The specimen configuration, and also the impedance set-up followed in the present investigation are similar to that employed by Andrade *et al.*[10–12]

Pore solution studies

As part of this study, a few cylindrical OPC and SRPC mortar specimens were cast in plastic bottles. The OPC and SRPC cylindrical mortar specimens were cast with similar mortar mixes and chloride levels as that of the corresponding electrochemical specimens. After placing and compacting the mortar, the plastic bottles were immediately sealed by wrapping with plastic sheet (Nesco film) to avoid interaction with the atmosphere. The sealed mortar specimens were then cured in a laboratory environment until the 70th day of hydration and were then subjected to pore solution extraction. This study was carried out to characterize the pore solution in mortar hydrated in an environment isolated from the atmosphere.

Pore solution was also extracted from the electrochemical mortar specimens on the completion of the electrochemical monitoring (about 70 days). For this purpose, the specimens were crushed and the crushed mortar fragments were then used for pore solution extraction. This study was necessary in order to build up a relationship between the electrochemical results and the pore solution characteristics.

The pore solution was extracted from the mortar by using a pore solution extractor (design pressure 375 MPa) using a method similar to that of Barneyback and Diamond.[13] The expressed pore solution was collected in a plastic syringe attached to the end of the plastic outlet of the extractor, and was then analysed for chloride and hydroxide ion concentrations.

The pH of the accurately diluted pore solution was measured immediately after extraction with a pre-calibrated pH probe, designed for high pH and with a low alkali error (Russel type W sensing glass). The measured pH values were then converted into the corresponding hydroxide ion concentrations in the pore solution by assuming unit activity coefficient. The free-chloride present in the appropriately diluted pore solution was measured on a pre-calibrated chloride analyser (Corning, model: 926). The measured chloride and hydroxide concentrations for the pore solution extracted

from the sealed specimens were not corrected for hydration effects, and thus, represent the actual concentration in the pore solution.

SEM and EDX analyses

A few mortar fragments ($\approx 10 \times 10 \times 10$ mm) were dried in laboratory air and then mounted, sputter-coated with carbon, and in few cases by gold, in order to provide a conductive surface. The coated surface of the specimen was then electrically connected to a brass mount by applying silver conductive paint. Microscopy was carried out on an Amray SEM (model 1810), and for qualitative analyses of the phases, an energy dispersive X-ray analysis (LINK) system attached to a SEM was used.

TEST RESULTS

Corrosion potentials for the steel electrodes in OPC and SRPC mortar specimens

Figure 2 presents the corrosion potentials as a function of curing period for both steel electrodes in OPC mortar specimens that contained different levels of chloride (0%, 1%, 1.75% and 3.5% chloride by weight of cement). Similarly, Fig. 3 presents the corrosion potentials for the steel electrodes in SRPC mortar specimens.

In Fig. 2, at around the 70th day of curing, the steel electrodes in mortar specimens that contained 0%, 1% and 1.75% chloride had all attained potentials of around -250 mV SCE, which may suggest passivation of the electrode surfaces, although the above observation alone cannot be taken as conclusive evidence of the passive state of the steel. The steel electrode number 1 (solid line) in the chloride-free mortar appears to attain a passive state at around the 12th day, while electrode number 2 (dashed line) demonstrates the attainment of passivity from the beginning. From the Fig. 2, it also appears that electrode number 2 (dashed line), which was embedded in mortar that contained 1% chloride, appeared to be in a passive state from the beginning. On the other hand, electrode number 1 (solid line) showed a large transition in its potential, from initially nobler potentials to active potentials at around the 17th day of hydration. On crushing the specimen at the end of the study, severe crevice corrosion attack on the electrode surface beneath the polymer–cement-based coating was observed. Thus, the shift in potential, as described above, is believed to be caused by this observed crevice corrosion attack. On the other hand, both the steel electrodes in mortar that contained 1.75% chloride took a relatively longer period (~ 70 days) to attain the typical passive potentials (~ -250 mV SCE) compared with the steel electrodes in mortar that contained 0% and 1% chloride. For both the electrodes in mortar specimens with 3.5% chloride, the potentials remained more negative

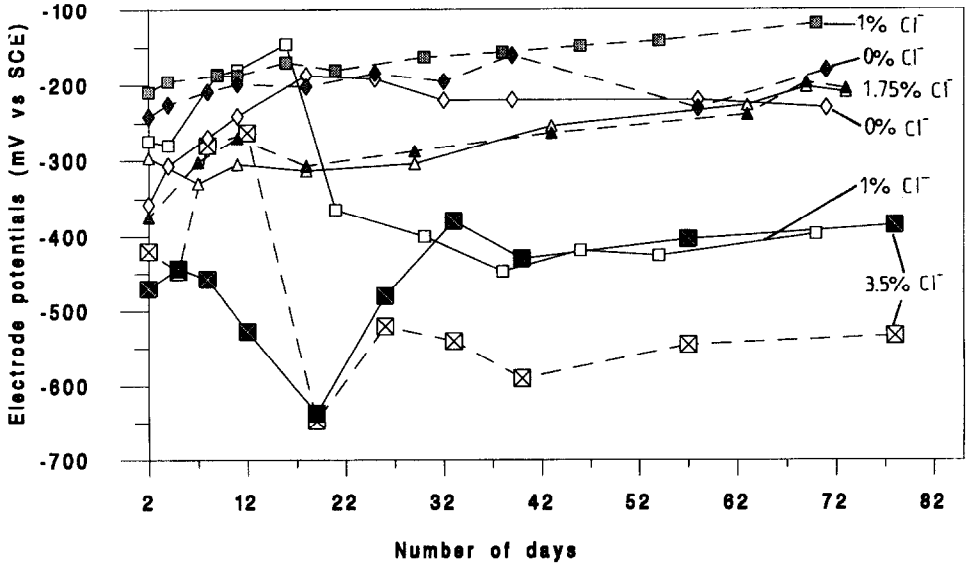

Fig. 2. Electrochemical potentials measured for the steel electrodes in OPC mortar specimens (key: solid line is for electrode number 1, and the dashed line is for electrode number 2).

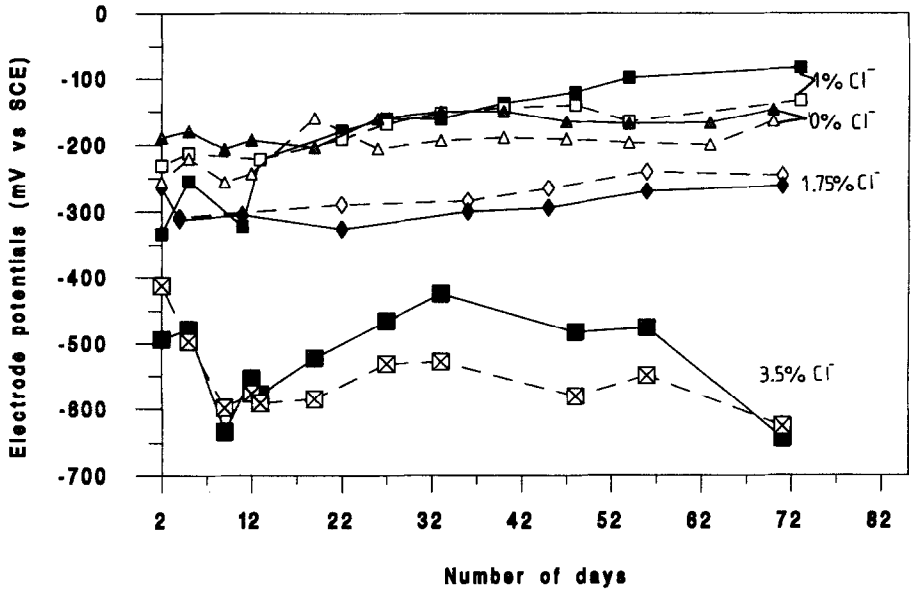

Fig. 3. Electrochemical potentials measured for the steel electrodes in SRPC mortar specimens (key: solid line is for electrode number 1, and the dashed line is for electrode number 2).

than −375 mV SCE from the beginning to the end (80 days) of curing, which suggests that active corrosion of the steel electrodes (e.g. pitting) initiated during the initial period, was still continuing at the completion of the experiment.

In Fig. 3, the steel electrodes in mortars that contained 0% and 1% chloride were in a passive state by the end of the curing period, while those in mortar that contained 1.75% and 3.5% chloride failed to attain passive potentials (~ −250 mV vs SCE) from the beginning of the curing period. From Fig. 3 it appears that both the steel electrodes in chloride-free mortar were in a passive state from the beginning. Similarly, electrode number 2 (dashed line) that was in mortar that contained 1% chloride seemed to be in a passive state from the beginning, while electrode number 1 (solid line) seemed to attain a passive state at around the 12th day of curing. Contrary to the steel electrodes in OPC mortar specimens with 1.75% chloride (Fig. 2), the steel electrodes in the SRPC mortar specimen that contained a similar level of chloride (1.75%), showed potentials that were more negative than −250 mV SCE from the beginning to the end (70 days) of the curing period. The behaviour of steel electrodes in SRPC mortar specimens that contained 3.5% chloride was similar to that of the steel in OPC mortar that contained 3.5% chloride. Thus, it appears that, the steel electrodes in SRPC mortar specimens that contained 1.75% and 3.5% chloride were actively corroding (e.g. pitting) from the beginning to the end of the curing period.

AC impedance measurements

Before commencing AC impedance measurements, the potentiostat that acted as an electrochemical interface in the 3-electrode circuit was checked for its ability to reproduce the voltage perturbation applied through the FRA, given the relatively high resistivity system. This was performed using a dummy cell that contained circuit parameters near to those expected for the steel–mortar interface.

In the following section, the AC impedance results are presented in the form of Cole–Cole, Bode and phase shift vs frequency plots. Cole–Cole and the conventional Nyquist plots resemble each other in appearance: in the former the real impedance is expressed using values from which the solution resistance (R_s) has been subtracted. The R_s in the present case is the uncompensated resistance between the tip of the reference electrode and the steel working electrode. The impedance results presented below correspond to the steel working electrode number 2, for which the corrosion potentials are shown by the dashed lines in Figs 2 and 3. In all the impedance plots presented below, the measured impedance values have been normalized to the area of the working electrode exposed to the mortar. This was done by multiplying the real and imaginary impedance

values obtained for all the frequencies by the exposed surface area of the steel electrode (9.2 cm^2).

Steel electrodes in chloride-free OPC and SRPC mortar specimens

In the present investigation it is assumed that the Randles circuit as shown in Fig. 4 represents the electrochemical interface formed at the steel–mortar interface.

The Cole–Cole, Bode and the phase shift vs frequency plots for the steel electrodes (electrode number 2) in chloride-free OPC and SRPC mortar specimens are presented in Figs 5 and 6 respectively. All the Cole–Cole plots presented in these figures resemble straight lines that are inclined slightly from the vertical axis, and indicate a general capacitive response. For the steel electrodes in both OPC and SRPC mortars, the phase angles show an increasing trend at higher frequencies; however, from about 1 Hz to ~ 10 mHz the phase angles were generally around 80°, which also indicates a capacitive response. The magnitude of this interfacial capacitance (C_{dl}), as estimated from

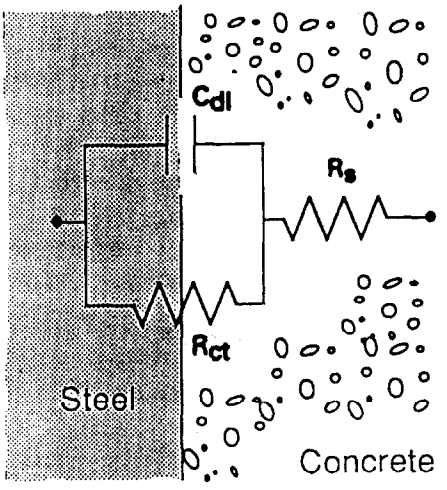

Fig. 4. A simple Randles circuit used to represent the steel–concrete interface.

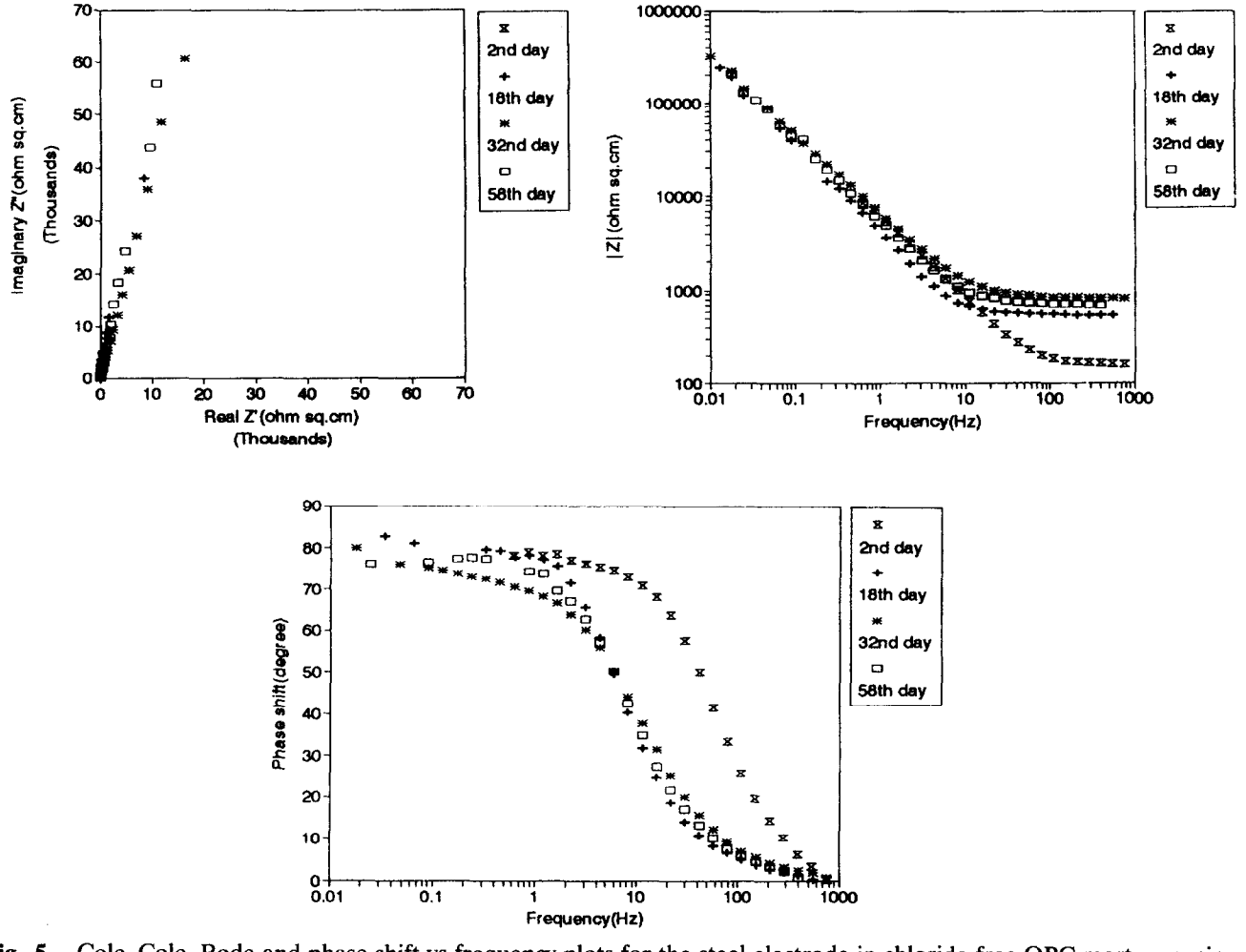

Fig. 5. Cole–Cole, Bode and phase shift vs frequency plots for the steel electrode in chloride-free OPC mortar specimen.

the experimental data, $[(C_{dl} = 1/\omega Z'')]$ were found to be nearly constant over the entire frequencies scanned. For example, for the steel electrode in chloride-free OPC mortar, the estimated values of C_{dl} were between 18 and 30 μf per cm^{-2} over the entire range of frequencies scanned. Thus, the electrochemical response presented in Figs 5 and 6 for the steel electrodes in chloride-free OPC and SRPC mortar is mostly caused by interfacial capacitance (C_{dl}), with no trace of charge transfer resistance (R_{ct}) even at lower frequencies. Such electrochemical behaviour of the steel electrode as described above is typical of a passive surface. Thus, the plots that appear in Figs 5 and 6 represent the passive steel electrode surfaces in chloride-free OPC and SRPC mortar from the beginning of the curing period. The measured corrosion potentials for the steel electrodes in chloride-free OPC and SRPC mortars (dashed line) from the beginning of the curing period were also typical of passive steel surface (Figs 2 and 3). Thus, the results from both AC impedance and electrochemical potential measurements consistently demonstrate the passive state of the steel electrodes in chloride-free OPC and SRPC mortar from the beginning to end of the curing period.

Steel electrodes in OPC mortars that contain chloride

The impedance results for the steel electrodes embedded in OPC mortar that contained 1% and 1.75% chloride by weight of cement are presented in Figs 7 and 8, respectively. Similar to the steel electrode in chloride-free OPC mortar (Fig. 5), the Cole–Cole plots in Fig. 7 (1% chloride) also appear as straight lines that are inclined from the vertical axis; however, these are relatively more inclined from the vertical axis compared with those in Fig. 5. The magni-

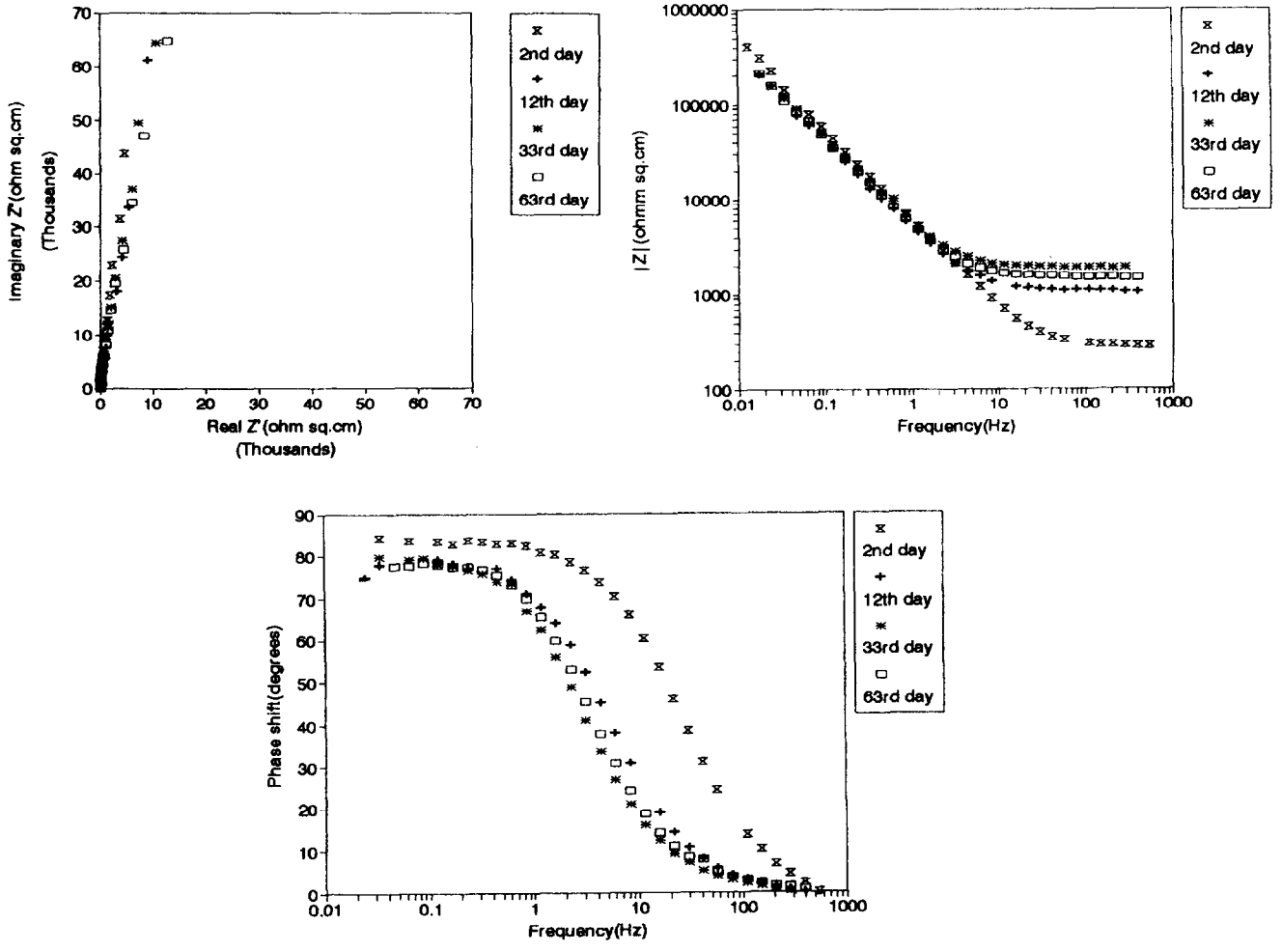

Fig. 6. Cole–Cole, Bode and phase shift vs frequency plots for the steel electrode in chloride-free SRPC mortar specimen.

tudes of the interfacial capacitance C_{dl} estimated from the experimental data were found to be nearly constant over the entire range of frequencies scanned. Further, they were also identical in magnitude to those for the steel electrode in chloride-free OPC mortar. Similarly the phase angle showed an increasing trend at higher frequencies, and at frequencies below 1 Hz the phase angles were nearly constant at around 70°. The measured potentials from the beginning to end of the curing period were typical of the passive steel surface (dashed lines in Fig. 2) and this evidence confirms that the steel electrode in OPC mortar with 1% added chloride is also in a passive state.

In Fig. 8 (1.75% chloride), the Cole–Cole plots are similar to those in Fig. 7; however, the plot for the 2nd day appears to be relatively more inclined from the vertical axis. Unlike the steel electrode in chloride-free OPC mortar, for the 2nd day of curing, the phase angle shows a decreasing trend below 1 Hz, and gradually drops to around 50° at around 50 mHz. Also the magnitude of impedance |Z| was slightly less at values of 0% and 1%, both of which were above 100 Ω cm^2. The measured potential for the 2nd day was also more negative than −350 mV SCE, which indicates active corrosion of the steel electrode. On the 18th, 29th and 69th days of curing, the phase angles below 1 Hz were generally between 60 and 70°. The measured corrosion potentials for the 18th and 29th days of curing were more negative than −250 mV SCE, and were so until around the 50th day: afterwards, they approached −200 mV SCE. Thus, based on the AC impedance results it is believed that the steel electrode embedded in mortar that contained 1.75% chloride was initially corroded (2nd day), and by the 69th day after further curing, the electrode surface is believed to be largely passive, with the possibility of pitting corrosion.

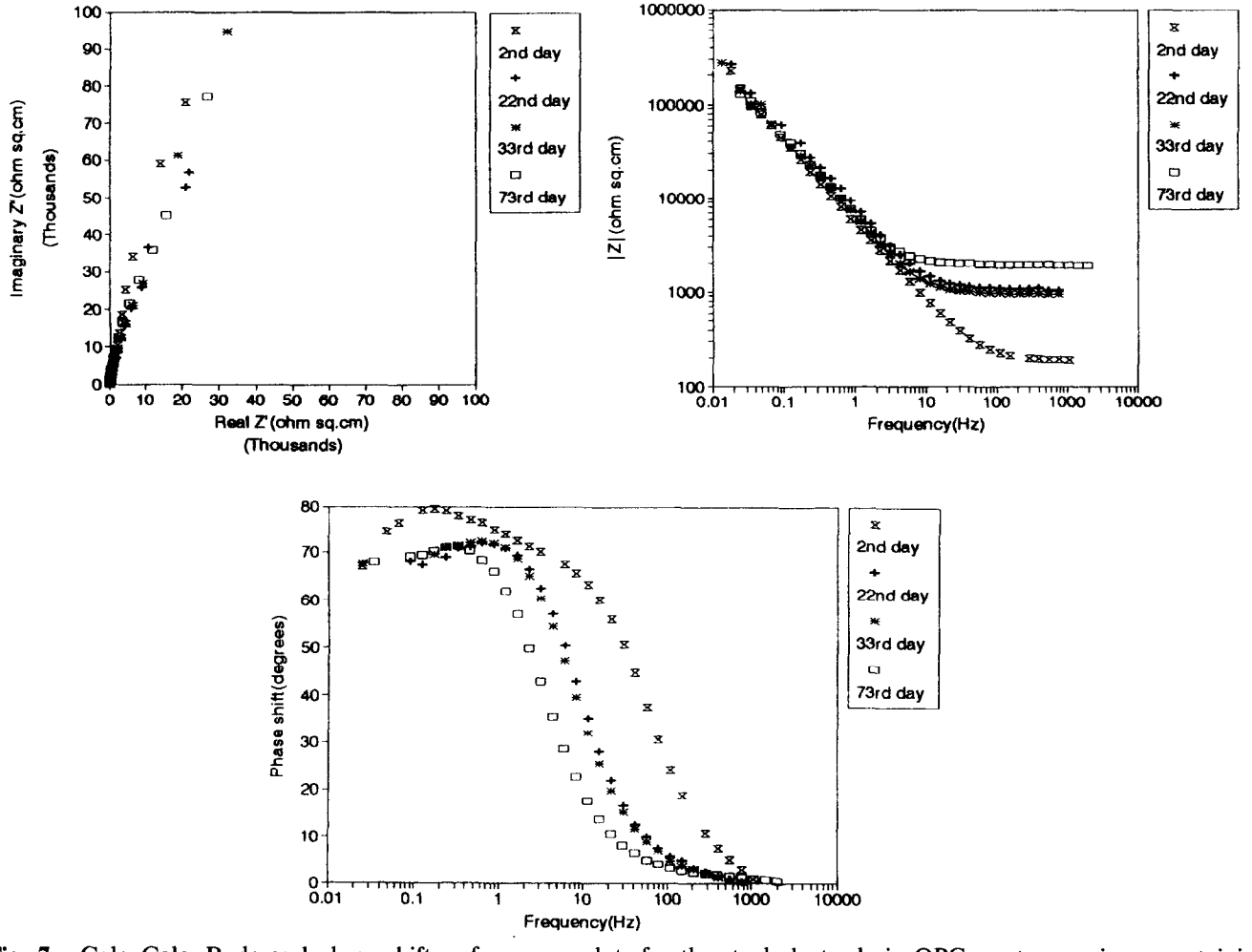

Fig. 7. Cole–Cole, Bode and phase shift vs frequency plots for the steel electrode in OPC mortar specimen containing 1% chloride by weight of cement.

Figure 9 presents the impedance results for the steel electrode in OPC mortar that contained 3.5% chloride. For this level of chloride, the Cole–Cole plots for all the days of curing appear as curves that are inclined significantly from the vertical axis. Moreover, contrary to the steel electrode in chloride-free OPC mortar, the phase angles below ~10 Hz for the 2nd day of curing, and below ~1 Hz for the 33rd, 57th and 70th days of curing were gradually decreased with frequency, to values between 20° and 50°. Also, contrary to the steel electrode in chloride-free OPC mortar, the magnitude of the capacitance estimated from the experimental data were found to vary over a wider range. The above evidence, together with the observation that the electrode potentials remained more negative than ~ −375 mV SCE over the entire curing period, suggest that the steel electrode in OPC mortar with 3.5% chloride was undergoing active corrosion from the beginning to the end of the curing period.

Steel electrodes in SRPC mortar that contained chloride

Figures 10 and 11 present the impedance results for the steel electrode in SRPC mortar that contained 1% and 1.75% chloride, respectively. Similar to the steel electrode in chloride-free SRPC mortar, the Cole–Cole plots for the steel electrodes in SRPC mortar with 1% chloride (Fig. 10) also appear as straight lines inclined from the vertical axis. However, the plots for the latter were relatively more inclined from the vertical axis compared with the former. Further, unlike the steel electrode in chloride-free SRPC mortar, the phase angles below ~10 Hz for the 2nd day, and below ~1 Hz for the 22nd, 36th and 71st days of curing, decreased with frequency to reach phase angles of around 60°. Also, contrary to the steel electrode in chloride-free SRPC mortar, the magnitudes of C_{dl} estimated from the experimental data were found to vary over a wider range. The above

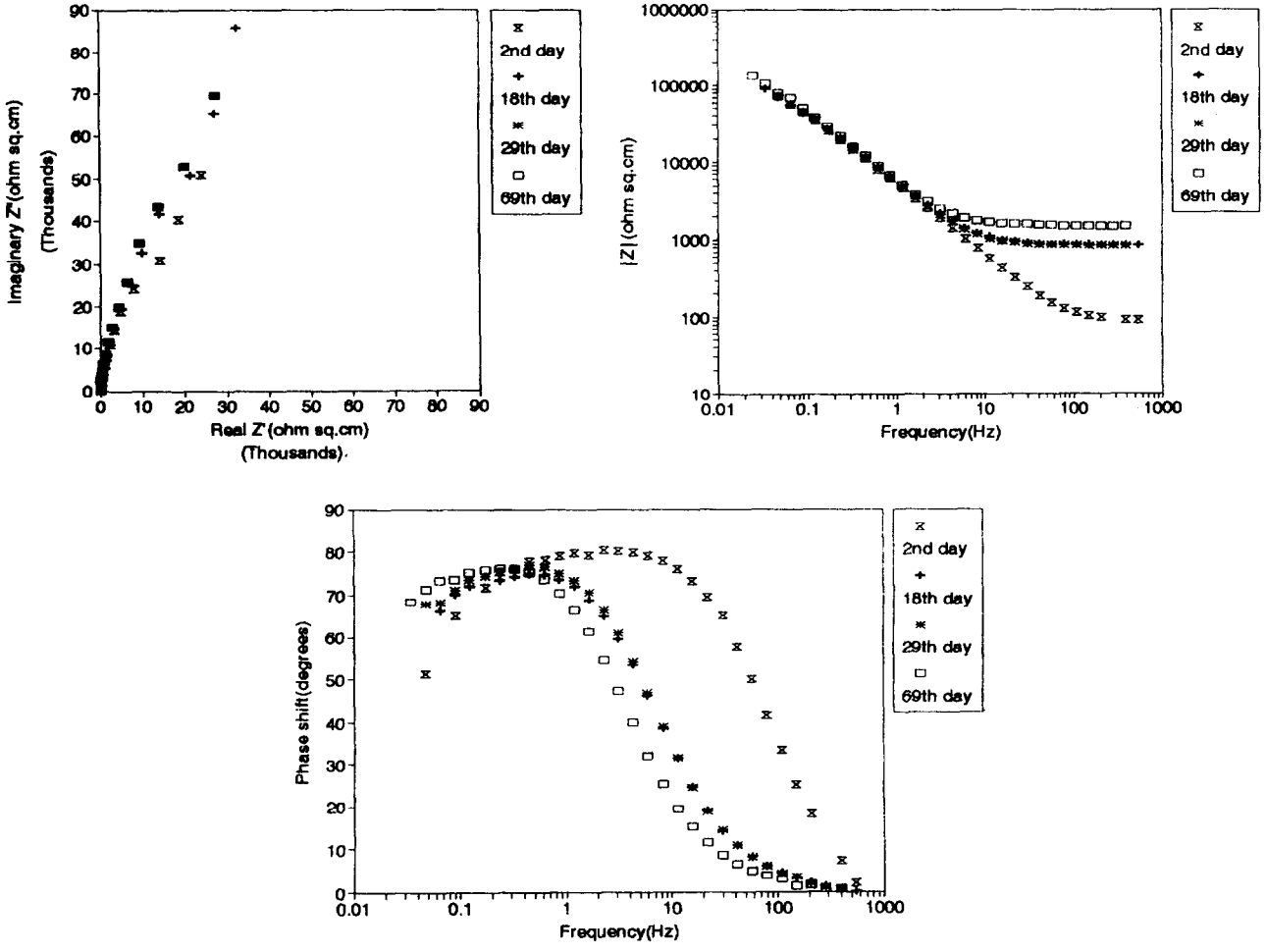

Fig. 8. Cole–Cole, Bode and phase shift vs frequency plots for the steel electrode in OPC mortar specimen containing 1.75% chloride by weight of cement.

results suggest pitting of the steel electrode surface. Thus, it is believed that the steel electrode underwent pitting over the entire curing period and the measured corrosion potentials were between −150 and −250 mV SCE.

The steel electrode in SRPC mortar with 1.75% chloride (Fig. 11) showed clear evidence of intensive pitting corrosion on the electrode surface. At the 2nd day of curing, the Cole–Cole plot resembled a partial semi-circle with phase shifts below ~1 Hz dropping gradually with frequency to a value as low as 40° (30 mHz). At the 11th day of curing, the Cole–Cole plot did not appear as a partial semi-circle; however, the phase shifts followed a similar trend as that for the 2nd day. At the 38th and 70th days of curing, the Cole–Cole plots appeared as straight lines inclined from the vertical axis; however, they were inclined relatively more from the vertical axis than those of the steel in chloride-free SRPC mortar. At the 38th and 70th days of curing, the phase angles below ~1 mHz decreased gradually with frequency and reached phase angles of around 60° (40 mHz). Contrary to the steel electrode in chloride-free SRPC mortar, for all the days of curing, the estimated C_{dl} values varied over a wider range as a function of frequency. The measured corrosion potentials were more negative than −250 mV SCE over the entire curing period. Thus, the above results demonstrate pitting of the steel electrode surface from the beginning of the curing period.

Although the impedance results for the steel electrode in SRPC mortar that contains 3.5% chloride are not presented here, the results were similar to Fig. 11, and pitting of the steel electrode surface was similar to the steel electrode in OPC mortar with 3.5% chloride.

Thus, from the above results it is evident that the steel electrode in chloride-free OPC and SRPC mortar attained passivity from the beginning. The steel electrode in OPC mortar with 1% chloride maintained passivity despite the

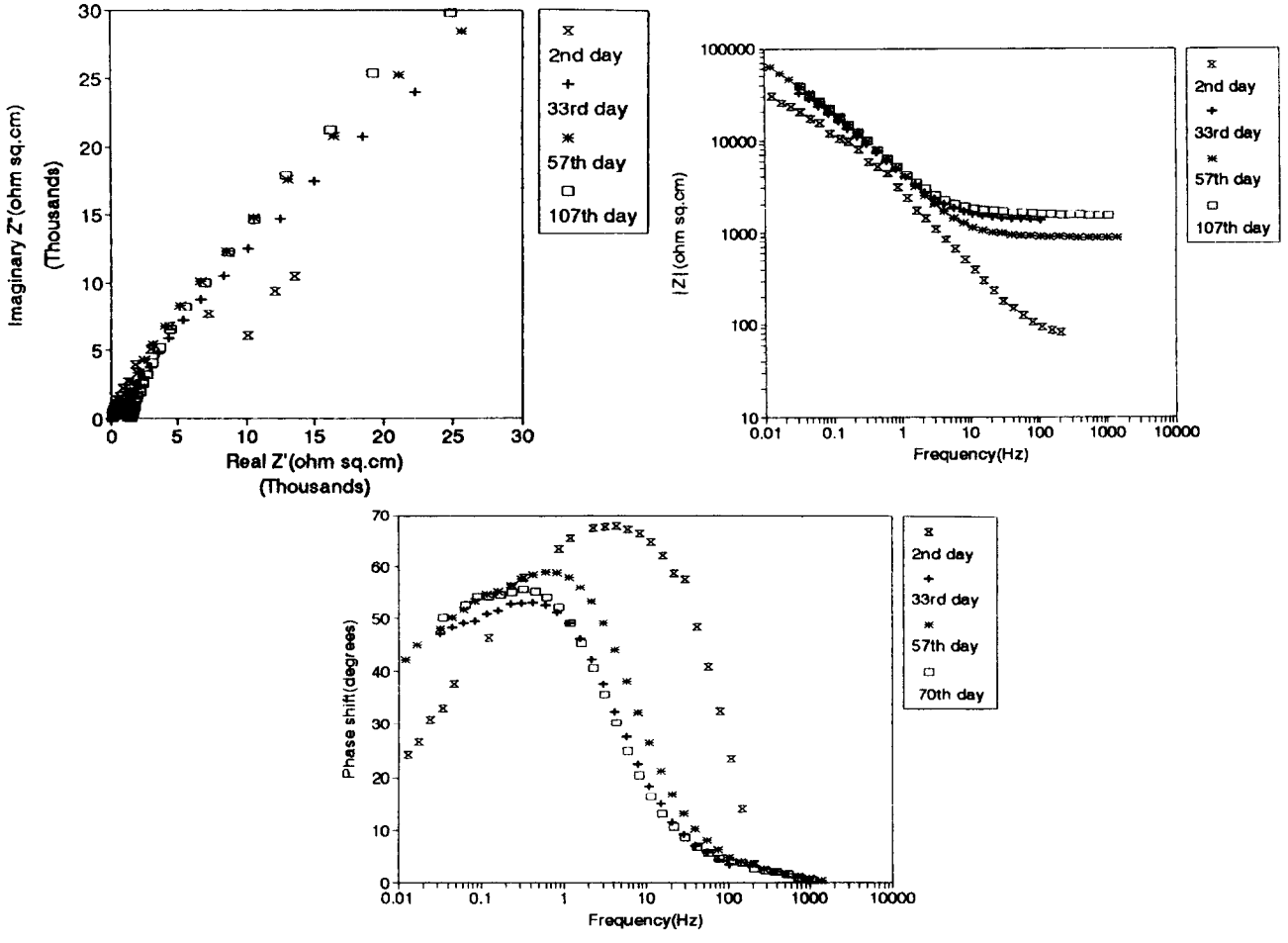

Fig. 9. Cole–Cole, Bode and phase shift vs frequency plots for the steel electrode in OPC mortar specimen containing 3.5% chlorides by weight of cement.

presence of 1% chloride in the mortar. However, addition of 1.75% chloride to the OPC mortar initiated pitting corrosion on the electrode surface. On the other hand, 1% chloride addition to the SRPC mortar was sufficient to initiate pitting on the embedded steel electrode from the beginning. Addition of chloride at 1.75% to SRPC mortar resulted in intensive pitting of the embedded steel electrode from the beginning. The addition of chloride of up to 3.5% resulted in severe corrosion of the steel electrodes embedded in both OPC and SRPC mortars from the beginning.

Characteristics of the pore solution extracted from the mortar specimens

Table 1 presents the free-chloride concentration, hydroxide ion concentration and the corresponding Cl^-/OH^- ratios for the pore solutions extracted from the OPC and SRPC electrochemical mortar specimens. Table 2 presents the above results for the pore solution extracted from the cylindrical OPC and SRPC mortar specimens hydrated in an environment isolated from the atmosphere.

For both 1% and 1.75% chloride levels, the pore solution extracted from the SRPC electrochemical mortar specimens (Table 1) had about two times higher free-chloride compared with the corresponding pore solution extracted from the OPC electrochemical mortar specimens. The above results demonstrate the higher chloride binding capacity of OPC compared with SRPC under unsealed condition. On the other hand, for both the chloride levels, the hydroxide ion concentration in the pore solution extracted from OPC and SRPC mortar specimens were nearly identical. Thus, for all the chloride levels, because of the higher free-chloride concentration, the resulting Cl^-/OH^- ratios for the SRPC mortar specimens were

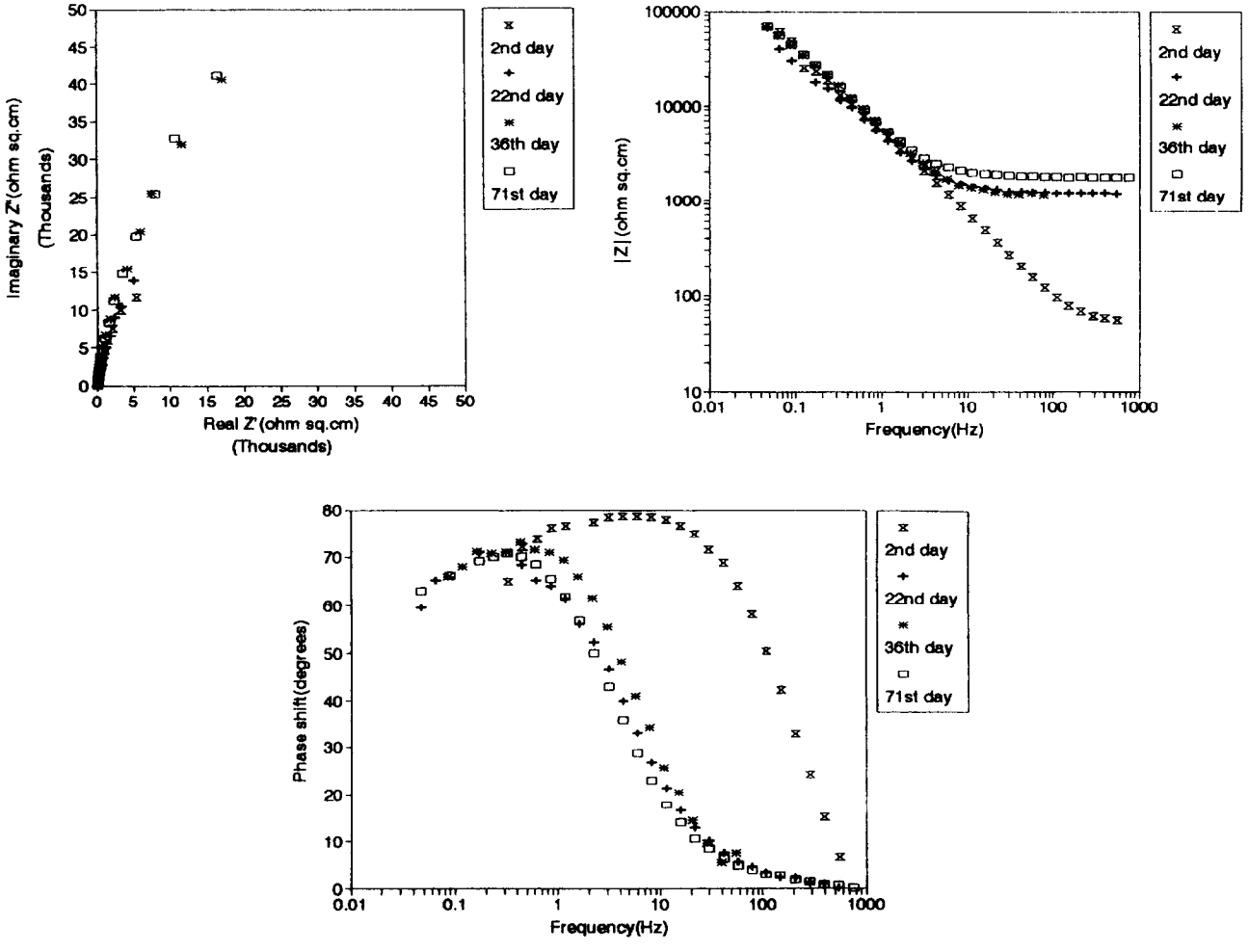

Fig. 10. Cole–Cole, Bode and phase shift vs frequency plots for the steel electrode in SRPC mortar specimen containing 1% chlorides by weight of cement.

almost two times greater than those for the corresponding OPC mortars.

For all the three chloride levels (1%, 1.75% and 3.5%) the pore solutions extracted from the SRPC-sealed mortar specimens (Table 2) consistently showed higher (1.3 to 1.7 times) free-chloride levels than the corresponding OPC-sealed mortar specimens. The above results demonstrate the lower chloride binding ability of SRPC compared with OPC when the mortars were hydrated in an environment isolated from the atmosphere. In contrast, the hydroxide ion concentration in the pore solution extracted from SRPC-sealed mortar specimens for all the chloride levels were consistently lower (1.5 times) than the corresponding sealed OPC mortar specimens. Thus, because of the combined effect of high free-chloride and low hydroxide ion concentration, the resulting Cl^-/OH^- ratios for the SRPC-sealed mortar specimens for all the chloride levels were more than twice that for the corresponding sealed OPC mortar specimens.

By comparing Table 1 and Table 2 it is evident that, the hydroxide ion concentrations for the OPC and SRPC electrochemical mortar specimens (unsealed) with 1% and 1.75% chloride levels are more than two times smaller than the corresponding OPC and SRPC cylindrical mortar specimens hydrated in sealed condition. In contrast, the free-chloride ion concentration in the pore solutions extracted from the OPC and SRPC electrochemical mortar specimens (unsealed), and the sealed OPC and SRPC mortar specimens, are nearly identical. Thus, because of the reduced hydroxide ion concentration, the resulting Cl^-/OH^- ratios for the OPC and SRPC cylindrical specimens in sealed condition are approximately two times lower than the corresponding OPC and SRPC electrochemical specimens.

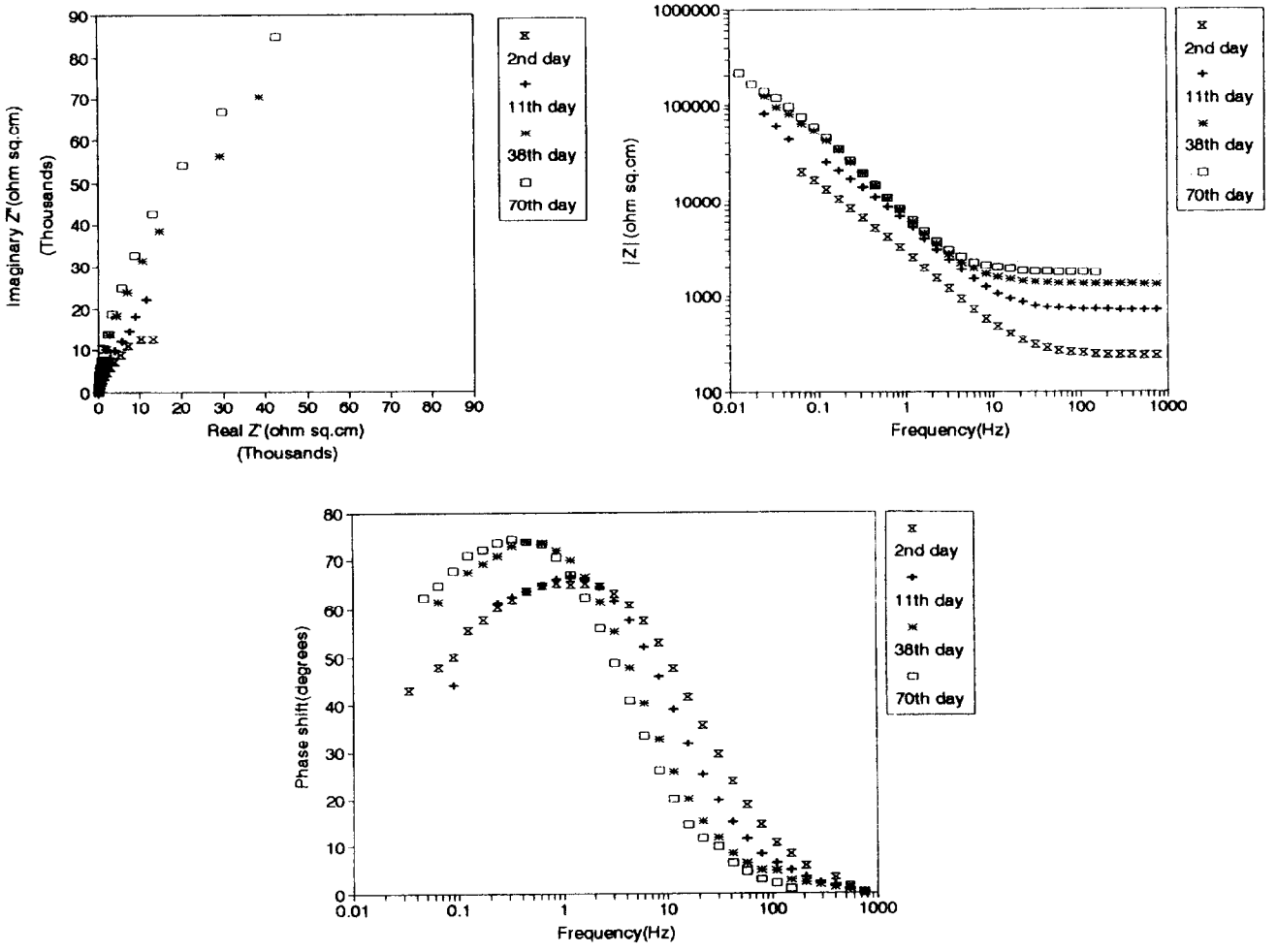

Fig. 11. Cole–Cole, Bode and phase shift vs frequency plots for the steel electrode in SRPC mortar specimen containing 1.75% chlorides by weight of cement.

Table 1. Cl^-/OH^- ratios for the OPC and SRPC electrochemical mortars (unsealed) that contain chlorides, as sodium chloride, after ~70 days of hydration

Specimen type	*Free-chloride conc. (M)*	*Hydroxide ion conc. (M)*	*Cl^-/OH^-*
OPC, 1% Cl^-	0.126	0.054	2.33
OPC, 1.75% Cl^-	0.318	0.084	3.57
SRPC, 1% Cl^-	0.257	0.052	4.94
SRPC, 1.75% Cl^-	0.599	0.067	8.94

SEM and EDX studies

The mortar fragments from both OPC and SRPC mortar specimens were examined under a SEM for the presence of Friedel's salt and its ferrite analogue.

The OPC mortar fragments when viewed under a SEM showed the presence of many hexagonal plate-like phases lying in the hydrated matrix as shown in Fig. 12. The EDX spectrum from X-ray spot analysis of the hexagonal plates at location marked A is shown in Fig. 13. The X-ray spectrum shows strong peaks for Ca (Ca-K_α, 1.49 KeV), Cl (Cl-K_α, 2.67 KeV) and a weak peak for Al (Al$-K_\alpha$, 1.49 KeV). Apart from the above, peaks for Si, Au and Fe (Fe$-K_\alpha$, 6.4 KeV) are also present in the spectrum. The peaks for Si and Fe are believed to be caused by a contribution from the matrix detected in the X-ray interaction volume. This is also supported by the fact that no compound in the form of hexagonal plates with the above composition (Ca, Cl, Al, Si and Fe) appears to exist in hydrated cement. Thus, it is strongly felt that the hexagonal plates are caused by Friedel's salt ($3CaO.Al_2O_3.CaCl_2.10H_2O$). The chloroferrite phase ($3CaO.Fe_2O_3.CaCl_2.10H_2O$) analogue to Friedel's salt present in SRPC mortar is shown in Fig. 14. The EDX spectrum from X-ray spot analysis of the hexagonal plates is shown in Fig. 15, which shows dominant peaks for Cl, Ca and Fe, and confirms the presence of the chloroferrite phase.

Thus, the above results confirm that the reduction in free-chloride concentration in the pore solution is caused by the chloride binding through Friedel's salt and its analogue chloroferrite phase in OPC and SRPC mortar, respectively, and thereby reduces the corrosion risk on the reinforcement steel.

In general, all the steel electrodes taken out from the specimens after crushing the specimen were found to be covered with a thin, dense white deposit layer, which is believed to be the cement hydration product. Figure 16 shows plate-like crystals of approximately 10 to 15 μm in thickness on the steel electrode from the OPC mortar specimen with 1% chloride. The EDX spectrum from X-ray spot analysis of the crystal in Fig. 17 shows a strong peak for Ca, which suggest the crystal is portlandite ($Ca(OH)_2$). Al Khalaf and Page[7] have also reported the formation of a dense layer of portlandite, which appeared as plate-like crystals on the surface of steel embedded in low w/c ratio cement pastes. Thus, it is concluded that the plate-like crystals observed in the present investigation are portlandite crystals.

Table 2. Cl^-/OH^- ratios for the OPC and SRPC sealed cylindrical mortar specimens that contain chlorides, as sodium chloride, after ~70 days of hydration

Specimen type	*Free-chloride conc. (M)*	*Hydroxide ion conc. (M)*	*Cl^-/OH^-*
OPC, 1% Cl^-	0.155	0.162	0.96
OPC, 1.75% Cl^-	0.332	0.199	1.67
OPC, 3.5% Cl^-	1.180	0.203	5.81
SRPC, 1% Cl^-	0.258	0.107	2.41
SRPC, 1.75% Cl^-	0.560	0.123	4.55
SRPC, 3.5% Cl^-	1.508	0.123	12.26

Fig. 12. SEM micro graph showing hexagonal plates of Friedel's salt present in OPC mortar containing chlorides (×5000). The bar indicates 10 μm.

DISCUSSION

A mortar mix of 0.70 w/c ratio was selected in the present study to simulate those situations where, because of lack of control, the actual w/c ratio of the mix exceeds the design w/c ratio of

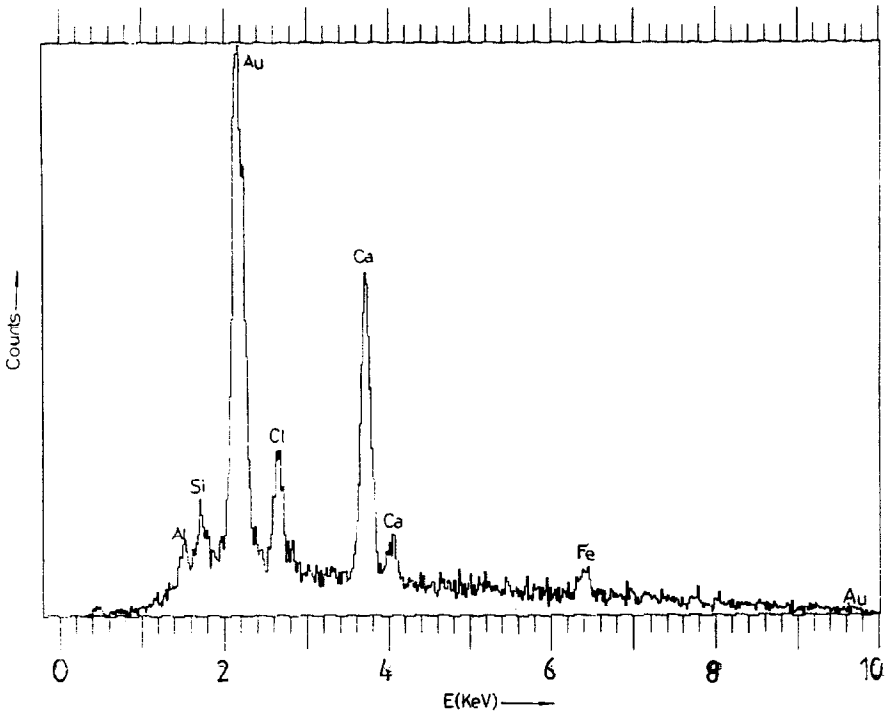

Fig. 13. EDX spectrum obtained from the X-ray spot analysis of Friedel's salt ($3CaO.Al_2O_3.CaCl_2.10H_2O$) at location A.

0.45. Despite the higher w/c ratio, the steel electrode in OPC mortar with chloride as high as 1% by weight of cement attained passivity from the beginning of the curing period. However, the steel electrodes in OPC mortar specimens with higher levels of chloride (1.75% and 3.5%), and those in SRPC mortar specimens at the above three different levels of chloride (1%, 1.75% and 3.5%) failed to attain passivity. Thus, despite the Cl^-/OH^- ratio of 2.33 (Table 1), the steel electrode in OPC mortar with 1% chloride attained passivity from the beginning of curing period that was similar to the steel electrode in chloride-free mortar. It is also evident that, the above threshold Cl^-/OH^- ratio is substantially higher than the threshold Cl^-/OH^- ratio of 0.61, as the limit for passivity of steel in saturated lime solution.[14] In the present study, the higher threshold Cl^-/OH^- ratio is also because of the use of polished steel electrodes instead of the 'as received' steel electrodes. The SEM study confirmed the formation of the lime-rich layer on the surface of the steel electrode embedded in OPC mortar with 1% chloride. By drawing inferences from Page's work it is believed that the observed large threshold Cl^-/OH^- ratio for the steel in the OPC mortar with 1% chloride is the result of a buffering mechanism in the lime-rich layer, which is shown to operate on the steel electrodes embedded in concrete of lower w/c ratio, and makes corrosion an anodically controlled process.[15] The lime-rich layer formed at the steel–mortar interface buffers the nearby pits by supplying hydroxide ions through its own dissolution. This raises the local pH to the saturation limit of the lime water, and thus, passivates the initially corroding pits. However, the repassivation of the pits through this buffering mechanism of the lime-rich layer is strongly dependent on the concentration of free-chloride present in the pore solution: beyond a certain

Fig. 14. SEM micrograph showing hexagonal plates of the chloro-ferrite phase ($3CaO.Fe_2O_3.CaCl_2.10H_2O$) in SRPC mortar containing chlorides (× 3380). The bar indicates 10 μm.

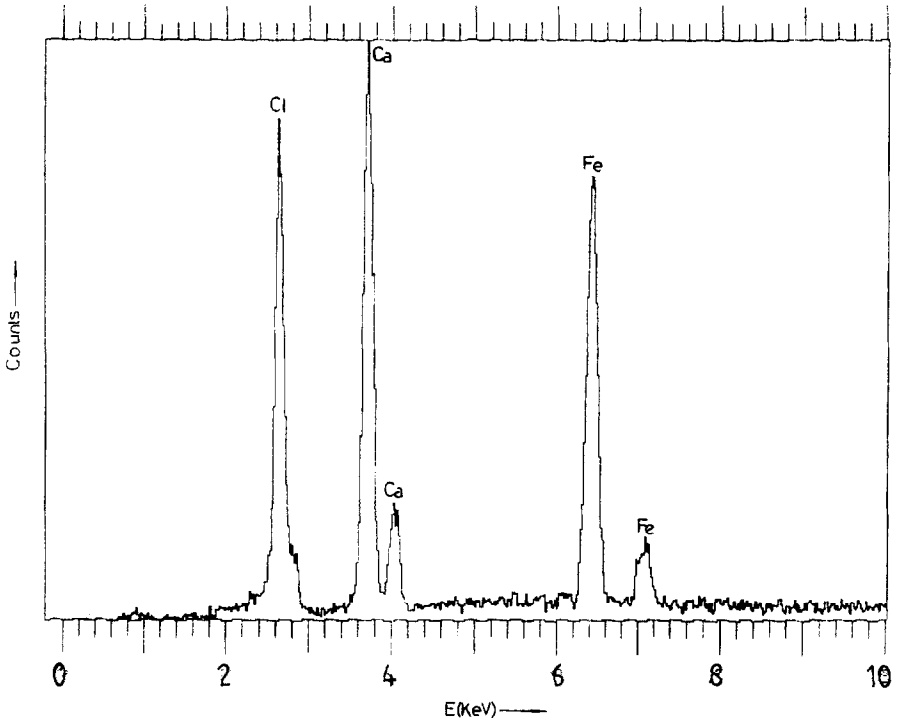

Fig. 15. EDX spectrum obtained from the X-ray spot analysis of the chloro-ferrite phase ($3CaO.Fe_2O_3.CaCl_2.10H_2O$).

threshold concentration of free-chloride, the buffering mechanism caused by the lime-rich layer becomes unable to preventing pitting. This explains the reason for the failure of the steel electrodes in OPC mortar, with 1.75% and 3.5% chloride, to attain passivity. On the other hand, with SRPC mortar, because of the high free-chloride concentration in the pore solution (Table 1), the resulting Cl^-/OH^- ratios for all the levels of chloride were significantly higher than those of the corresponding OPC mortar specimens. In other words, for the SRPC mortar, even with 1% chloride, the possibility of repassivation of the electrode surface by the buffering mechanism of a lime-rich layer, was beyond its scope. The higher free-chloride concentration in the pore solution obtained from the SRPC mortar was caused by the lower chloride binding ability of SRPC because of its to lower C_3A content. Despite the lower C_3A content of the SRPC, some chloride was still bound in the form of a chloroferrite phase (Fig. 14) analogue to Friedel's salt, because of the tetra-calcium aluminoferrite (C_4AF) content of the cement.

Fig. 16. SEM micrograph showing portlandite layer formed around the steel electrode in OPC mortar containing 1% chlorides by weight of cement ($\times 4070$). The bar indicates 5 μm.

The above discussion points out conclusively that, despite the mortar mix being a 0.70 w/c ratio, the special protection mechanism as proposed by Page was still operative in cement mortars whose C_3A content was as high as 11.2% (e.g. OPC). However, despite these findings, the authors do not recommend the use of a high w/c ratio OPC mortar/concrete mixes in situations where chloride contamination (internal chloride) is expected. In the event of chloride contamination in the mix, the current code requirement for relatively lower w/c ratio (0.45) mixes is sensible, and should be followed, since it produces concretes with dense pore structures. It is worth noting that, contrary to the situation in mortar/concretes of lower w/c

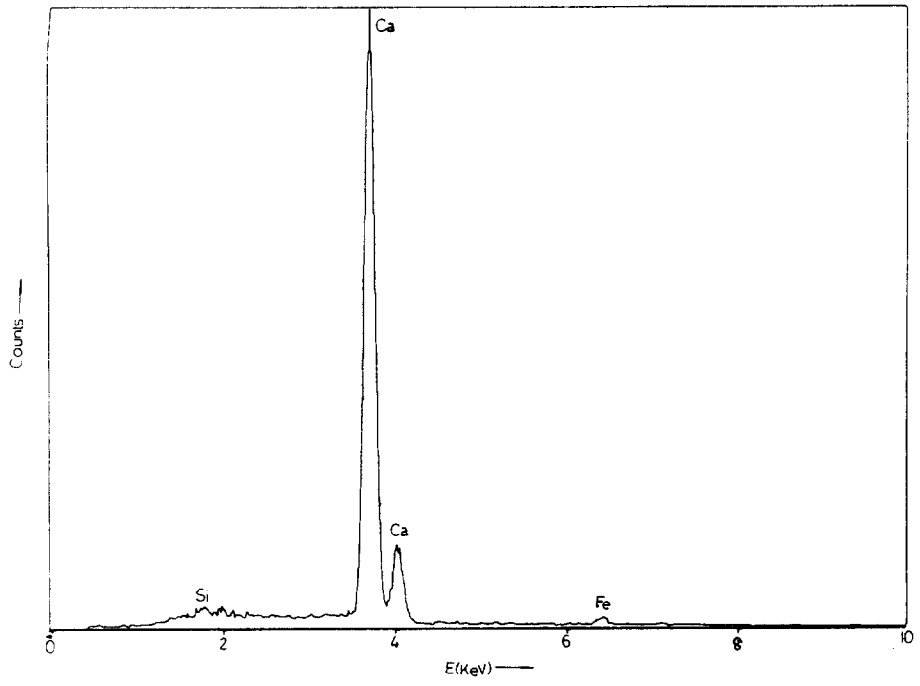

Fig. 17. EDX spectrum obtained from the X-ray spot analysis of the portlandite layer.

ratios, in a mortar mix of high w/c ratio, the mobility of free-chloride through the capillary pores is less restrained because of the presence of a coarse pore structure. Thus, in the case of a high w/c ratio concrete/mortar, there is a greater possibility for the unhindered supply of free-chloride to move to the corroding pit from the bulk, and thus, render the buffering mechanism ineffective earlier. On the other hand, in the case of a concrete/mortar of low w/c ratio (e.g. 0.45), the mobility of chloride is significantly restrained because of the constricted capillary pores. This will favour restriction of chloride supply from the bulk to the corroding pit on the steel surface and thus, indirectly favour the buffering mechanism.

A comparison between Table 1 and Table 2 clearly indicates the relatively large Cl^-/OH^- ratios for the OPC and SRPC electrochemical specimens compared with the corresponding OPC- and SRPC-sealed specimens. This was caused by the hydroxide ion concentration in the pore solution extracted from the OPC and SRPC electrochemical specimens that were unsealed from the atmosphere. The concentration was approximately two times smaller than that for the OPC and SRPC cylindrical mortar specimens that were hydrated in an environment isolated from the atmosphere. This indicates the strong effect of the Cl^-/OH^- ratio, in similar types of mortar, on the type of exposure (e.g. exposure to atmosphere). On the other hand, the type of exposure does not seem to influence the free-chloride concentration in the pore solution (Table 1 and Table 2). This suggests that the Cl^-/OH^- ratios evaluated from the mortar/concrete specimens cured in an environment isolated from the atmosphere are not appropriate for field concrete structures that undergo atmospheric carbonation attack.

The significant drop in hydroxide ion concentration in the pore solution extracted from both OPC and SRPC electrochemical mortar specimens is caused by the combined effects of higher w/c ratio of the mortar mix, and a RH below 100% that prevails in the cover region of the mortar specimen during the curing period. The carbonation of concrete reaches an optimum rate when the RH prevailing in the cover is around 50%[16] because of the increased air permeability of the concrete, and at beyond 80% RH, the rate of carbonation drops drastically.[17] In the present case, although the specimens were aged in a humidity chamber that was maintained at around 85% RH, it is believed that the RH prevailing in the cover region was still favourable for slow carbonation. The periodic withdrawal of the specimens from the humidity chamber for electrochemical monitoring, which lasted a few hours, is also believed

to have favoured intermittent moderate drying of the mortar and enhanced the penetration of atmospheric carbon dioxide (CO_2) into the cover region.

CONCLUSIONS

The following conclusions are derived from the present experimental investigation.

1. The steel electrodes in chloride-free OPC and SRPC mortar mixes of 0.70 w/c ratio attained passivity from the beginning of the curing period.
2. Despite the higher w/c ratio (0.70) of the mix, the steel electrodes in OPC (11.2% C_3A) mortars with chloride levels as high as 1% by weight of cement, also attained passivity. However, steel electrodes in OPC mortar with 1.75% and 3.5% chloride by weight of cement underwent corrosion attack. On the other hand, the steel electrodes in SRPC (1.4% C_3A) mortar at a similar w/c ratio to the above Cl levels (1%, 1.75% and 3.5%), were subjected to corrosion attack. Thus, the steel embedded in mortar cast with a cement of high C_3A content, even when the w/c ratio was higher than that normally recommended in codes, passivated in the presence of 1% chloride by weight of cement.
3. The hydroxide ion concentration in the pore solution is strongly dependent on the type of the exposure conditions that the mortar undergoes, for example, exposure of the mortar to the atmosphere. On the other hand, the type of exposure, such as the above, does not seem to have any influence on the free-chloride concentration in the pore solution.
4. Because of the atmospheric carbonation attack, the Cl^-/OH^- ratios for the OPC and SRPC mortar hydrated in an unsealed condition were approximately two times higher than the corresponding mortars hydrated in an environment isolated from the atmosphere. Thus, the Cl^-/OH^- ratios evaluated through mortar specimens hydrated in a sealed condition are not appropriate for field structures that undergo atmospheric carbonation attack.
5. The OPC of higher C_3A content binds larger amounts of free-chloride than SRPC of low C_3A content under identical conditions, and thus demonstrates the significance of the C_3A phase of the cement.
6. The chloride in OPC mortar binds in the form of Friedel's salt ($3CaO.Al_2O_3.CaCl_2.10H_2O$), which can be seen as hexagonal plates under a SEM. On the other hand, the chloride in SRPC mortar binds less effectively in the form of a chloroferrite phase, ($3CaO.Fe_2O_3.CaCl_2.10H_2O$), analogous to Friedel's salt, which also can be seen as hexagonal plates under a SEM.
7. Similar to steel in concrete or mortar of low w/c ratio, a lime-rich layer of approximately 10–15 μm in thickness forms on a steel electrode that is embedded in a mortar mix of w/c ratio as high as 0.70. The special corrosion protection mechanism as suggested by Page is also valid for steel embedded in mortar with a w/c ratio as high as 0.70.

ACKNOWLEDGEMENTS

The first author would like to thank The Commonwealth Commission in the UK for the financial assistance provided to carry out his Ph.D degree at UMIST, Manchester during September 1991 to September 1994.

REFERENCES

1. Rasheeduzzafar, X., Al-Saadoun, S. S., Al-Gahtani, A. S. & Dakhil, F. H., Effect of tricalcium aluminate content of cement on corrosion of reinforcing steel in concrete. *Cem. Concr. Res.*, **20** (1990) 723–738.
2. Suryavanshi, A. K., Scantlebury, J. D. & Lyon, S. B., The binding of chloride ion by sulphate resistant Portland cement. *Cem. Concr. Res.*, **25** (1995) 581–592.
3. Rasheeduzzafar, X., Influence of cement composition on concrete durability. *ACI Mater. J.*, **89** (1992) 574–586.
4. Rasheeduzzafar, X., Ehteshan Hussain, S. & Al-Saadiun, S. S., Effect of cement composition on chloride binding and corrosion of reinforcing steel in concrete. *Cem. Concr. Res.*, **21** (1991) 777–794.
5. Holden, W. R., Page, C. L. & Short, N. R., The influence of chlorides and sulphates on durability. In *Corrosion of Reinforcement in Concrete Construction*, Crane, A.P. (Ed.). Ellis Harwood Ltd, England, pp. 143–150.
6. Dehganin, C. & Lock, C. E., Effect of chloride ion type on corrosion of steel in concrete. Proc. 8th Int. Congress on Metallic Corrosion, 1981, II, pp. 1761–1766.
7. Al Khalaf, M. N. & Page, C. L., Steel/mortar interfaces: Microstructural features and mode of failure. *Cem. Concr. Res.*, **9** (1979) 197–208.
8. Treadaway, K. W. J., Cox, R. N. & Brown, B. L., Durability of corrosion resisting steels in concrete. Proc. Institution of Civil Engineers, Part I, 1989, April, Vol. 86, pp. 305–331.
9. Zhang, S. H. & Lyon, S. B., Problems in AC impedance measurement of high resistance system in

thin-film electrolytes. IEE Colloquium, Digest 071, Proc. Institution of Electrical Engineers, London, 1994.
10. Andrade, C. & Castelo, V., Practical measurement of the AC impedance of steel bars embedded in concrete by means of a spectrum analyser (fast Fourier transform). *Br. Corros. J.*, **19** (1984) 98–100.
11. Andrade, C., Castelo, V., Alonso, C. & Gonzalez, J. A., The determination of the corrosion rate of steel embedded in concrete by the polarisation resistance and AC impedance methods. ASTM STP 906, American Society for Testing and Materials, Philadelphia, 1986, pp. 43–63.
12. Alonso, C. & Andrade, C., Effect of nitrite as corrosion inhibitor in contaminated and chloride-free carbonated mortars. *ACI Mater. J.*, **87** (1990) 130–137.
13. Barneyback, R. S. & Diamond, S., Expression and analyses of pore fluids from hardened cement pastes and mortars. *Cem. Concr. Res.*, **11** (1987) 279–285.
14. Hausman, D. A., Steel corrosion in concrete: How does it occur?. *Mater. Protect.*, **6** (1967) 19–23.
15. Lambert, P., Page, C. L. & Vassie, P. R. W., Investigation of reinforcement corrosion. 2 Electrochemical monitoring of steel in chloride-contaminated concrete. *Mater. Struct.*, **24** (1991) 351–358.
16. Gjorv, O. E., Mechanisms of corrosion of steel in concrete structures. *Proc. Eval. Mater.*, **89** (1989) 565–578.
17. Parrot, L. J., Influence of environmental parameters upon permeability: A review. Permeability of concrete as criterion of its durability, Report of RILEM Technical Committee 116-PCW, RILEM, France, 1990.